Open Access

Recent Progress in Materials

LIDSEN Publishing Inc.

Original Research

Low-Velocity Impact Resistance of Glass Laminate Aluminium Reinforced Epoxy (GLARE) Composite

Abolfath Askarian Khoob [1], Mohammad Javad Ramezani [1], Seyed Sina Mousavi [2,*]

1. Dept. of Mechanical Engineering, Imam Khomeini naval academy, Nowshahr, Iran; E-Mails: askariankhoob@gmail.com; m.javad.ramezani.0068@gmail.com
2. Dept. of Civil Engineering, Babol Noshirvani University of Technology (BNUT), Babol, Iran; E-Mail: ssmousavi@nit.ac.ir

* **Correspondence:** Seyed Sina Mousavi; E-Mail: ssmousavi@nit.ac.ir

Academic Editor: Luciano Ombres

Special Issue: Fiber Composite Materials and Civil Engineering Applications

Recent Progress in Materials
2023, volume 5, issue 2
doi:10.21926/rpm.2302021

Received: June 16, 2022
Accepted: May 08, 2023
Published: May 12, 2023

Abstract

This study intends to determine the behavior of glass laminate aluminum-reinforced epoxy (GLARE) and glass fiber-reinforced polymer (GFRP) composites under a low-velocity impact test. Experimental tests and numerical simulations are considered for this investigation. All samples are made by the hand lay-up method. Moreover, specimens are produced with a 7075-T6 aluminium sheet with a 0.5 mm thickness, resin 3001, and E-glass fiber. The drop weight test performs the low-velocity impact at 6.7 J and 10 J impact energy levels and the heights of 1.0 m and 1.5 m. Numerical simulation is also conducted by ANSYS software to compare the results obtained by the experimental tests. Generally, results show that maximum deflections of the GLARE samples are significantly lower as compared to GFRP ones by 87% and 83.5% for 1.0 m and 1.5 m drop heights, respectively. Experimental results demonstrate that although aluminum sheets prevent damage to the fibers in GFRP, delamination and fractures between layers are observed in GFRP samples. An appropriate agreement is also obtained between the FE results and experimental data.

Keywords
GLARE; composite; FML; GFRP; low-velocity impact; drop weight test

1. Introduction

Previous studies have been made many efforts to determine the performance of composite materials in the past decades [1]. The main concern in composite materials is to reduce the weight of the plates and maintain reliable strength, which has led to weight loss in structural design. Generally, composites have many advantages over metal alloys, especially in cases where specific strength and stiffness are required. However, the performance of composite materials under impact loading is usually weaker than that of metals. The need to improve the impact behavior of polymer composites has led to the development and introduction of a new generation of composites, denoted as fiber-metal laminates (FMLs) composites. FMLs are classified into hybrid composite materials that consist of thin metal sheets and fiber-reinforced polymer layers. The fiber-reinforced layers commonly used in the FMLs are glass-reinforced, carbon-reinforced, basalt-reinforced, and kevlar-reinforced composite. The metal alloy sheets are aluminum, magnesium, titanium, or stainless steel. Three commercially available FMLs based on a thin sheet of Al alloy and epoxy-based composite layers. In this field, glass laminate aluminum reinforced epoxy (GLARE) composite comprises glass fiber reinforced laminate. Similarly, CARALL and ARALL composites comprise carbon fiber-reinforced laminate and aramid fiber-reinforced laminate, respectively.

Generally, aluminum alloy-based fiber metal laminates are widely used in aircraft structures because of their good fatigue, impact resistance, and high weight-saving potential. Therefore, the 2000 and 7000 series of aluminum alloy-based FMLs are used in industrial applications such as aerospace and automotive structures. Due to the good mechanical properties and corrosion behavior of FMLs composites, many studies recommend using this composite type in the marine industry, offshore, and underwater applications [2-7]. Laminated structures perform very well against the rapid growth of fatigue cracks [8]. Many studies determined the mechanical properties, classification, and manufacturing process of FMLs [8-11]. In this field, Ding et al. [9] and Logesh et al. [2] focused on the fabrication processes of FMLs and forming technologies, especially stamp forming. Vermeeren [10] reviewed the history of ARALL and GLARE applications in the aerospace industries. Also, the effect of significant factors on the mechanical properties of FMLs was studied by Chandrasekar et al. [11] in alignment with investigating the impact of temperature and humidity. Along with valuable investigations on the mechanical characteristics of FMLs, some important experimental studies based on scattered databases worked on impact resistance, especially low-velocity impact properties [12-16]. Based on the conflicting findings in this field, more experimental works must be confirmed by researchers. Moreover, the present work intends to address this issue due to a research gap in the literature regarding low-velocity impact resistance of GLARE compositecompared to the GFRP plate. In this context, Sinmazcelik et al. [17] investigated the different test methods of FML, such as bending, tensile, fatigue, and impact. Sadighi et al. [18] reviewed the impact resistance of fiber-metal laminates. They examined various impact resistance parameters, such as material selection, and some simulation and impact loading methods on FMLs samples. A comprehensive review was conducted by Chai & Manikandan [8] on the low-velocity

impact response of fiber-metal laminates. In this field, Azhdari et al. [3] investigated the low-velocity impact response of GLAREs based on experimental and numerical studies. They found that increasing impact energy increases the number of cracks and damage in the samples. Furthermore, with increasing impact energy, the fibers break, and the plastic deformation of the aluminum layer becomes the predominant damage state. Bienias et al. [4] studied low-velocity impact resistance on fiber-metal laminates based on experimental and FE simulations. In the experimental method, 1.5-3.5 mm thick fiber-metal composite samples made from aluminum sheets and glass/epoxy are produced and tested using an autoclave process. Low-velocity impact experiments were performed with 10-joule and 25-joule impact energies. They found that the main sheet damage includes delamination occurring in the composite layers and the metal-composite interface, and cracks in the composite and lower metal layers. Also, their findings revealed that modeling of impact in fiber metal sheets using VUMAT code allows us to assess the damage to their structure and choose the appropriate laminate configuration in the future regarding their resistance to low-speed impact. Morinière et al. [5] investigated damage rates in GLARE composites with low-velocity impact tests. They analyzed the samples using visual inspection, chemical etching, and C-scan, and the damage history was reconstructed from the observations of this experimental study. Their results showed that the excellent resistance of GLARE composite specimens to impact caused by glass/epoxy layers delayed aluminum perforation. The aluminum sheets prevented severe damage, projectile penetration, and delamination growth. Yaghoubi et al. [6] investigated the effects of the thickness of the GLARE composite and projectile mass under a low-velocity impact test. Their results showed the amount of energy absorption increased by increasing the thickness of the composite samples. Also, with the reduction of the projectile's mass but maintaining the same impact energy, the deflection of the middle point and the amount of damage increased so that the specimens were perforated. Rajkumar et al. [7] studied the behavior and mechanical degradation of fiber-metal laminates under the low-velocity impact test. Their results showed that impact energy, failure strain, and peak load decreased by increasing the number of impacts due to composite sample damage. Furthermore, great damage, deformation, delamination, and even cracking of aluminum sheets were found in FML composites with increasing impacts on the samples. Zhang et al. (2018) [19] presented an analytical model based on a modified rigid-plastic material approximation to study the low-velocity impact of fully clamped sandwich beams with FML face sheets and metal foam core struck by a heavy mass. Similarly, Zhang et al. (2021) [20] investigated the low-velocity impact of square FML sandwich plates through analytical and numerical methods. In this field, Zhang et al. (2022) [21] experimentally and numerically studied the dynamic response of aluminum honeycomb sandwich plates with GLARE face sheets. They found that the deformation mode of the sandwich plate was on the front face sheet. Moreover, they reported that by increasing the face-sheet thickness, maximum deflection and energy absorption of the back face-sheet decreased. In this context, Zhang & Guo (2021) [22] used theoretical analysis and FE simulation to study the dynamic response of rectangular foam-filled FML tubes, based on the modified rigid-plastic material approximation. Their results show that as the metal volume fraction in FMLs, the number of metal layers in FML, and the foam strength increased, the force decreased. Additionally, they found that the number of metal layers in FMLs substantially influences the force-deflection and initial impact energy-maximum deflection.

Although some studies concentrated on the low-velocity impact resistance of FMLs composites, there is no specific study to compare the performance of FMLs (hereafter called GLARE) with glass

fiber reinforced polymer (GFRP) composite. Moreover, their research did not precisely consider modal analysis to determine the natural frequency of the GLARE composite along with impact resistance. Hence, in the present study, 7075-T6 aluminum alloy FML (GLARE) is introduced to make the tiers of enclosed superstructures of large ships that are not exposed to seawater. However, falling equipment may impact the floor of the enclosed superstructure's tiers. Thus, the impact behavior of GLARE is experimentally studied by a drop weight test. The effects of two different drop heights and the same dimensions on the GLARE and GFRP specimens are studied. The key parameters considered in the present study are absorbed energy, maximum impact loading, and midpoint displacement. Furthermore, finite element (FE) analysis by ANSYS software is performed to anticipate the behavior of GLARE and GFRP specimens under the impact test. Modal analysis is also conducted by experimental, numerical, and analytical methods to compare the natural frequency of GLARE and GFRP composites. Four initial modes of composites are compared.

2. Experimental Procedure

2.1 Materials

Aluminum alloy 7075-T6 sheets with a thickness of 0.5 mm are used as the metal component of the GLARE composite fabrication. The properties of the aluminum 7075-T6 sheet (with a thickness of 0.5 mm) are mentioned in Table 1. The type T6 sheet has a higher yield strength because the primary source of this strength mainly depends on the dispersion and deposition time between the grains and along the grain boundary, and the resistance to stress corrosion decreases. The [0/90] woven E-glass fabric (with the trade name QUANTOM Wrap 200G) and epoxy resin (QUANTOM EPR 3001) are used as the composite parts of the GLARE composite fabrication. This epoxy resin has many advantages, such as high mechanical properties, resistance, impact, and excellent adhesion between inner layers of glass fiber, especially aluminum sheets. The mechanical properties of the GFRP composite according to the ASTM D3039 and ASTM D4255 standards are shown in Table 2. The mechanical properties are obtained from GFRP composite laminates due to recent research conducted in this composite laboratory [23, 24]. Furthermore, the mechanical characteristics of the epoxy resin are presented in Table 3.

Table 1 Properties of aluminum 7075-T6 alloy.

Properties	Value
E (GPa)	71.7
G (GPa)	26.9
ν	0.33
ρ (kg/m^3)	2700

Table 2 Mechanical Properties of GFRP plates [23, 24].

Properties	Value
$E_{11} = E_{22}$ (GPa)	36
E_{33} (GPa)	7.6
$\nu_{12} = \nu_{23} = \nu_{13}$	0.25

$G_{12} = G_{13} = G_{23}$ (GPa)	2.6
ρ (Kg/m^3)	1615

Table 3 Characteristics of the resin 3001 [25].

Resin material	Density (kg/m^3)	color	Bonding strength (MPa)	Compressive strength (MPa)	Tensile and Flexural strength (MPa)
QUANTOM EPR 3001	1150	Grey	>1.8	60	>25

2.2 Manufacture of GLARE

The schematics of the samples are shown in Figure 1. Since the material selection and quality of GLARE and GFRP composite laminates produced in the experimental results are very important, making high-quality and uniform composite samples is very important. In this study, the hand lay-up method produced GFRP and GLARE composites . The mechanical process prepares aluminum surface and improve its adhesion to the composite. In the preparation of aluminum plates, first, they are washed, then wastes are separated from the surfaces of aluminum sheets and then degreased with acetone solution. Then, the inner surfaces of aluminum (the surfaces attached to the composite) are sanded until they are made a surface with deep scratches. The sanded surface is placed in boiling water for 20 minutes to form the OH^- and OH^+ factors on the surface. Also, the inner surface of aluminum sheets is scratched due to better adhesion between the aluminum sheets and glass fibers. In the resin preparation section to produce GLARE and GFRP samples, the resin is added to the hardener at a weight ratio of 3:1 and mixed with a mechanical stirrer for 10 minutes. In this part, after preparing the aluminum layers with dimensions of 25 × 25 cm and a thickness of 0.5 mm, four square pieces of 25 × 25 cm size are cut from the E-glass fiber. Eventually, four composite specimens were fabricated, including two GLARE composite specimens and two GFRP composite specimens. The thickness of the samples is 1.8 and 2.8 mm, respectively, as shown in Figure 2. The hand lay-up process is used to manufacture the 6-layer E-glass\epoxy composites. The GLARE specimens are manufactured by adding two 0.5 mm thick aluminum sheets, one on each side of GFRP laminate, shown in Figure 1. For the drop weight low-velocity impact test, four specimens are prepared with dimensions of 250 × 250 mm, which are 1.8 mm thickness for the GFRP laminates (two specimens), and 2.8 mm thickness for GLARE laminates (two samples), shown in Figure 2.

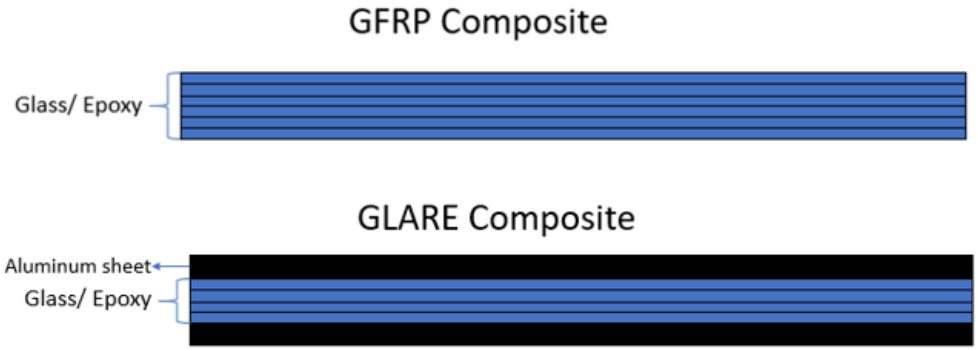

Figure 1 Schematic of GLARE and GFRP composite layering.

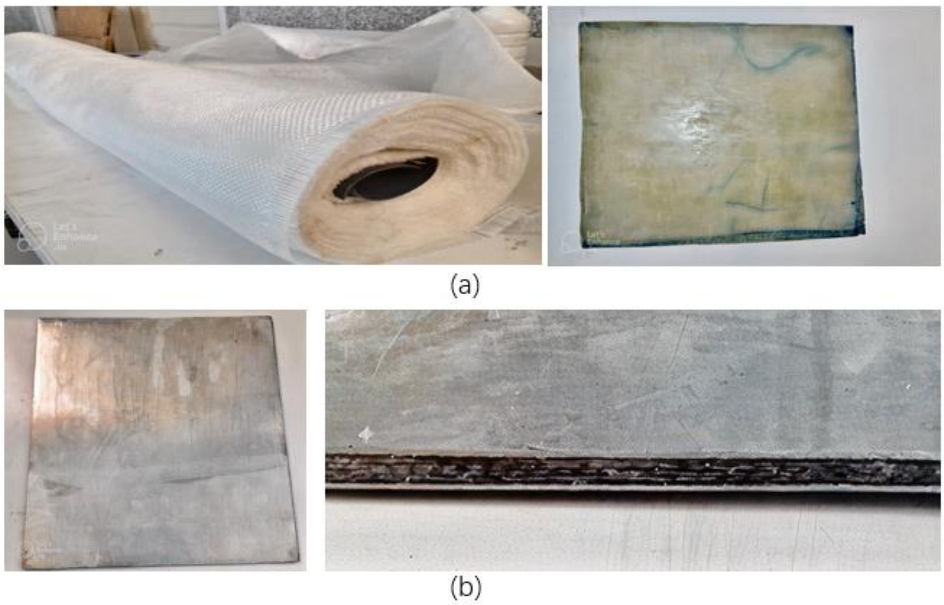

Figure 2 Composites: (a) GFRP; (b) GLARE.

2.3 Low-velocity Impact Test

This study uses a drop-weight test device with a spherical impactor to carry out low-velocity impact tests. The mechanism consists of an electric magnet. The task of the electric magnet is to hold the spherical projectile and the clamped boundary condition for composite samples. Furthermore, a laser displacement measuring and contact force measuring system are placed under the GLARE and GFRP composite laminates to record the maximum deflection value and contact force of the middle point of the specimens. As illustrated in Figure 3, an instrumented drop-weight impact machine with a controllable-drop height is used for the impact tests. The sample is clamped at the bottom of the machine between the two rectangular plates with a square opening at its center (Figure 4). The low-velocity impacts are performed with a spherical steel projectile with a diameter of 55 mm and a mass of 680 g, as shown in Figure 4. The laser displacement measurement is calibrated before performing the impact test. It should be noted that calibrating the sensor reduces the error rate to obtain the maximum amount of maximum deflection. The impact test is performed at a height of 1.0 m with a collision velocity of 4.46 m/s with an impact energy of 6.7 j and a height of 1.5 m with a collision velocity of 5.46 m/s with an impact energy of 10 j.

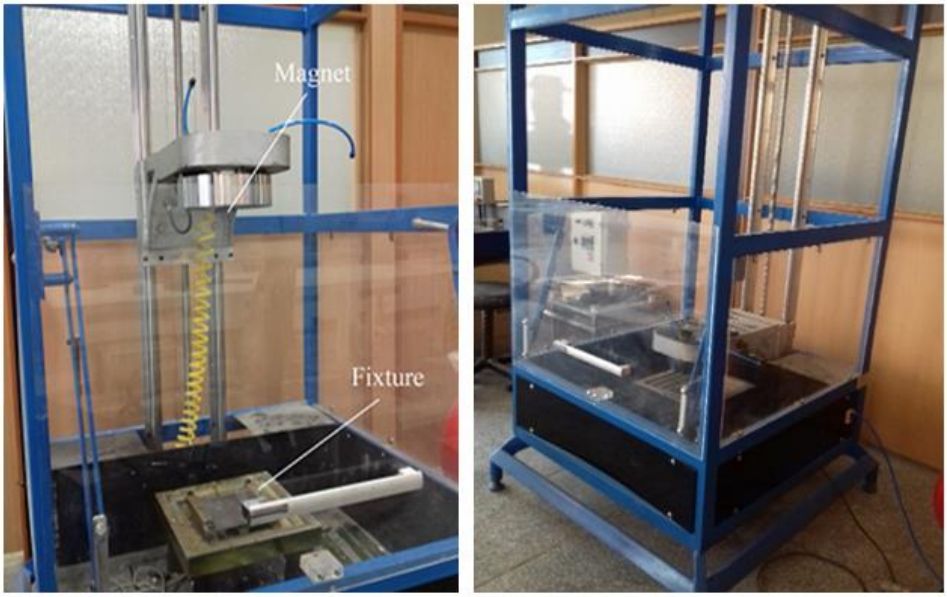

Figure 3 Drop weight impact machine set-up.

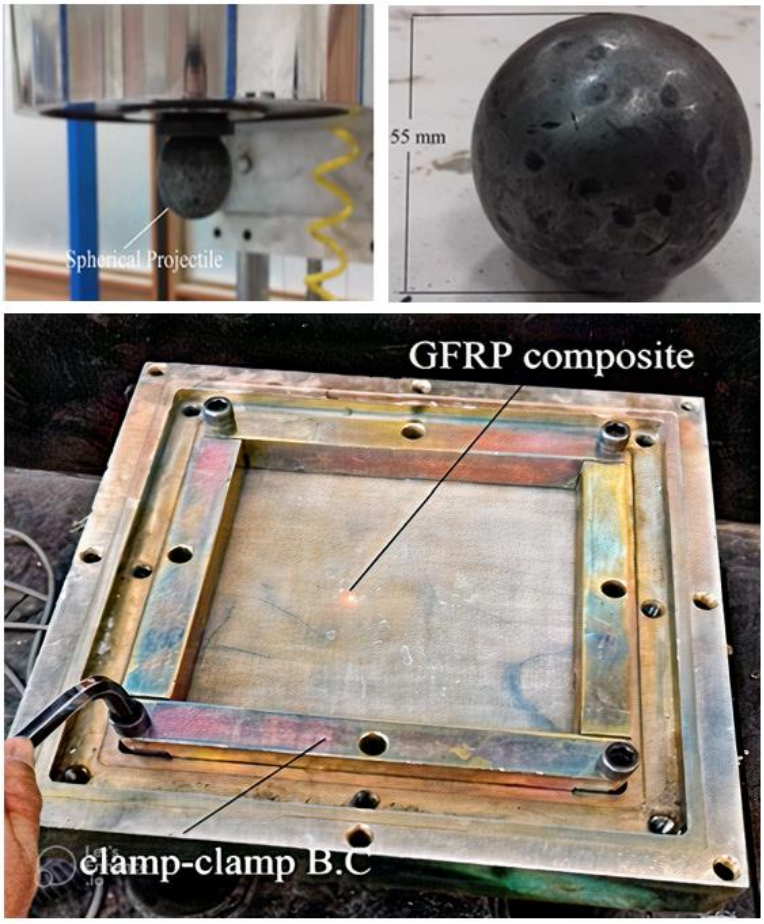

Figure 4 Spherical projectile and fixture.

2.4 Modal Analysis (Natural Frequency)

The modal test was performed to determine the natural frequencies in the modal laboratory. The equipment of this laboratory for achieving the desired test includes exact sensors, a hammer, a shaker, a system, and vibrating software to perform the test and receive frequency response. After setting up and installing the equipment and connecting the device to the software, composites were hung in an entirely free border condition using a thread to get the frequencies and shapes of the modes. The sensor is then attached to the sample by a magnet and struck with a hammer (Figure 5).

Figure 5 Experimental set-up to conduct modal analysis.

3. Numerical Simulation

A three-dimensional model of the specimen and impactor is applied in the Ansys LS-Dyna software to simulate the FML composite under low-velocity impact loading, as shown in Figure 6. The purpose is to evaluate the maximum deflection of the middle point of the GLARE and GFRP composites under dynamic loading. The 8-node element with three degrees of freedom at each node is selected to simulate the aluminum sheets and GFRP laminates. This element is only used in explicit dynamic analyses. A fully clamped boundary condition is applied to the specimens. Tables 1 & 2 show the isotropic properties of the aluminum sheets and the orthotropic properties of composite laminates used in the model, respectively. To simulate, the projectile and the composite samples are meshed by an 8-node solid element. The spherical projectile is assumed to be a rigid object without any deformation. In addition, the composite laminates have meshed with regular and fine sizes to achieve more accurate results. It should be noted that the more regular and integrated the mesh, the more precise the final answer. To simulate the contact behavior between projectile and composite laminates, the surface-to-surface automatic contact algorithm is selected

with the static coefficient of friction and dynamic coefficient of friction, which are 0.2 and 0.15, respectively [24]. The interlayer bond is destroyed if the interlayer stress (shear or normal) between the two adjacent layers exceeds the joint's normal or shear strength. The surface-to-surf-tied/fail contact algorithm models the composite samples to express the connection concept. Furthermore, when the contact stress between the composite layers does not reach normal or shear strength limits, the contact limit is removed, and the layers are separated. The projectile's initial velocity is the same as the velocities given in the experimental test section, which are 4.42 m/s and 5.42. Shear and tensile strength values are equal to 100 MPa and 30 MPa, respectively, between the contact layers of composite laminates [23]. According to Figure 6, all models are modeled as 1/2 to reduce the problem and solve it more. Similarly explained in the literature [26, 27], Hashin failure criteria [28] were considered in the present FEM study to model the failure of composite layers. Four different damage initiation mechanisms are used in these criteria: fiber tension, fiber compression, matrix tension, and matrix compression.

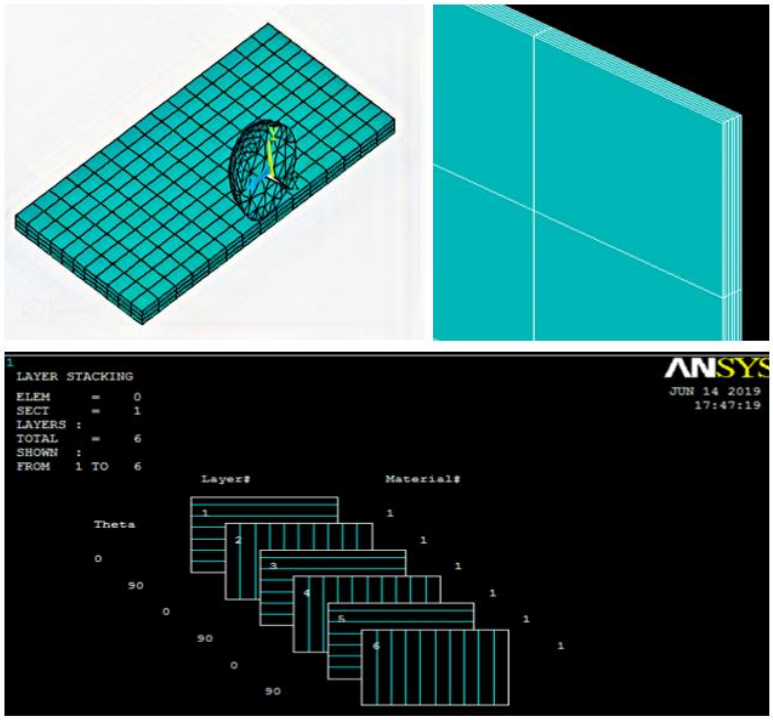

Figure 6 FE simulation of composites under impact loading.

4. Results and Discussion

4.1 Impact Test

In this section, the results obtained from experimental tests and FE simulation by ANSYS software are compared to investigate the behavior of GLARE and GFRP composite specimens under low-velocity impact. The first discussion is about the force-displacement curves of composites, shown in Figure 7(a). Experimental results show that the maximum deflection (midpoint) of the GLARE composites is significantly lower than GFRP composites so an 87.1% and 83.5% decrease were observed for impact energies of 6.7 j and 10 j, respectively (Figure 7(b)). As impact energy increases, midpoint deflection slightly increases. Moreover, results indicate that GLARE composites have

higher impact loading than GFRP ones, up to 10% and 13.6% enhancement for impact energies of 6.7 j and 10 j, respectively (Figure 7(c)). The area under the force-displacement curve shows the impact of absorbed energy by the composites, which is a critical parameter in controlling the ductility of the composites. As illustrated in Figure 7(a), the absorbed energy (area under the curve) of GFRP composite is significantly higher than GLAR composites due to the higher stiffness of GLARE composites, reducing the appropriate ductility. The presence of aluminum sheets reduced the deflection rate of GLARE samples compared to GFRP. Another factor that led to the decrease in deflection rate in the samples is the thickness. By increasing thickness, the amount of deformation and deflection is decreased. GLARE specimens' force-deflection history seems symmetric and shows the elastic-plastic response.

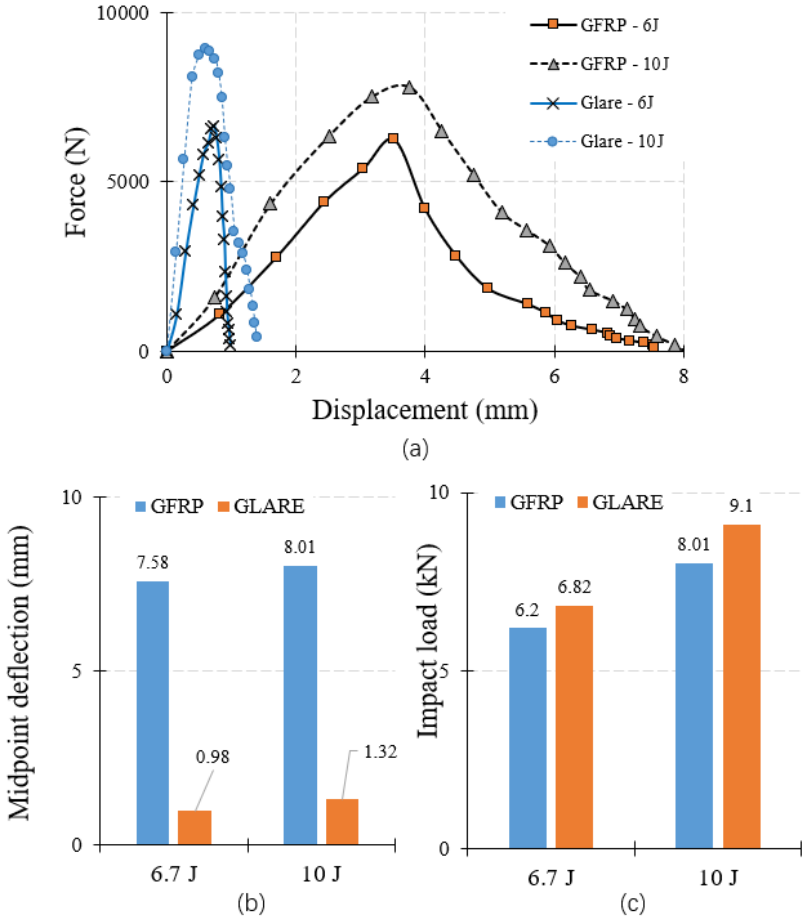

Figure 7 Experimental results of the impact test.

4.2 Natural Frequency

Experimental results obtained by the modal analysis show that the natural frequency of GLARE composites is significantly higher than GFRP ones. The natural frequencies of the first four modes of GLARE composites are 191.3 Hz, 312.5 Hz, 358.1 Hz, and 438.1 Hz. These values are 41.5 Hz, 101.1 Hz, 161.2 Hz, and 190.4 Hz for GFRP composites. Adding aluminum sheets considerably increases the stiffness of the composites, resulting in higher frequencies. The first four modes of composites are illustrated in Figure 8. Results show that changing the samples' thickness and stiffness changes the modes of the plates so that none of the first modes matches each other.

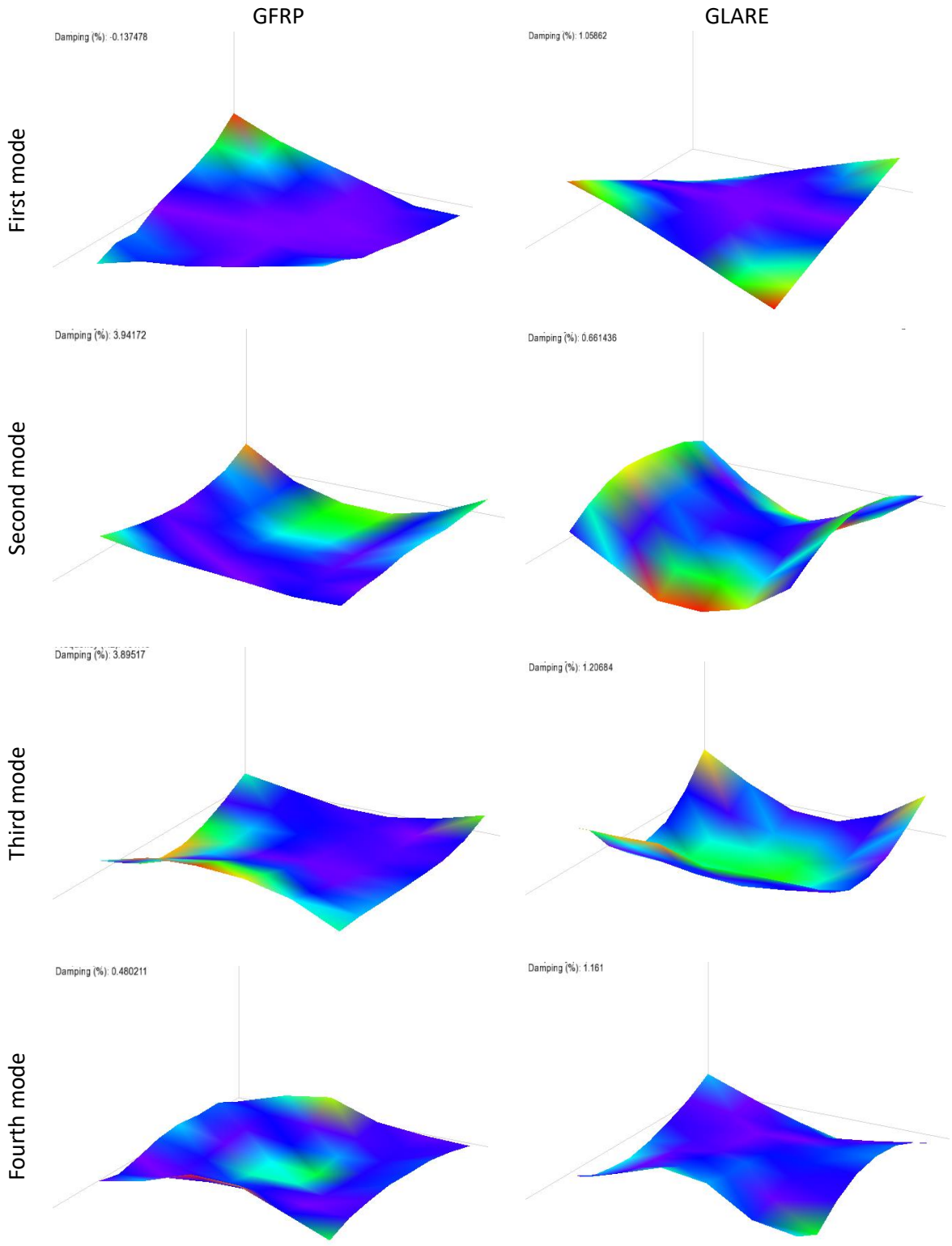

Figure 8 The first four modes of the composites induced by experimental tests.

4.3 Numerical Results

Numerical results for GFRP and GLARE composites under the impact test are summarized in Table 4, for two heights of 1 and 1.5 m with an impact speed of 4.42 and 5.42 m/s, respectively (impact energy of 6.7 J and 10 J). The maximum deflection of the middle point and the impact load of

specimens are compared in Table 4. Regarding midpoint deflection, results show less than 10% deviation exists between the experimental and numerical results of GFRP composites, with more than 10% error for GLARE composites. Similarly, results of impact load show that numerical simulation for modeling GFRP composites results in a lower deviation between experimental and numerical results than GLARE composites. Results show that the reason for the difference in the experimental and simulation results graph is the existence of voids in samples, laboratory temperature, and environmental and experimental construction conditions. The comparison curves are shown in Figures 9-12. In Table 4, the low thickness of GFRP samples has the most considerable deflection. In the case of the spherical projectile impact in the experimental method, the projectile hit the composite samples with skewed impacts in some instances. As a result, the spherical projectile surface has no complete contact with the laminate. Unlike the experimental method, the contact between the projectile and the laminates is generally completed in the finite element in samples. Consequently, there is a slight difference between experimental and FE data.

Table 4 Experimental and numerical results for GFRP and GLARE composites.

Specimen Type	Drop Height (m)	Impact energy (j)	Midpoint Deflection (mm)			Impact Load (KN)		
			FEM Solution	Experimental result	Error (%)	FEM Solution	Experimental result	Error (%)
GFRP	1.0	6.7	8.03	7.58	5.60	6.22	6.2	0.3
GFRP	1.5	10	8.60	8.01	6.80	8.02	8.01	0.1
GLARE	1.0	6.7	1.57	0.98	37.5	6.25	6.82	8.3
GLARE	1.5	10	1.82	1.32	27.5	8.90	9.10	2.1

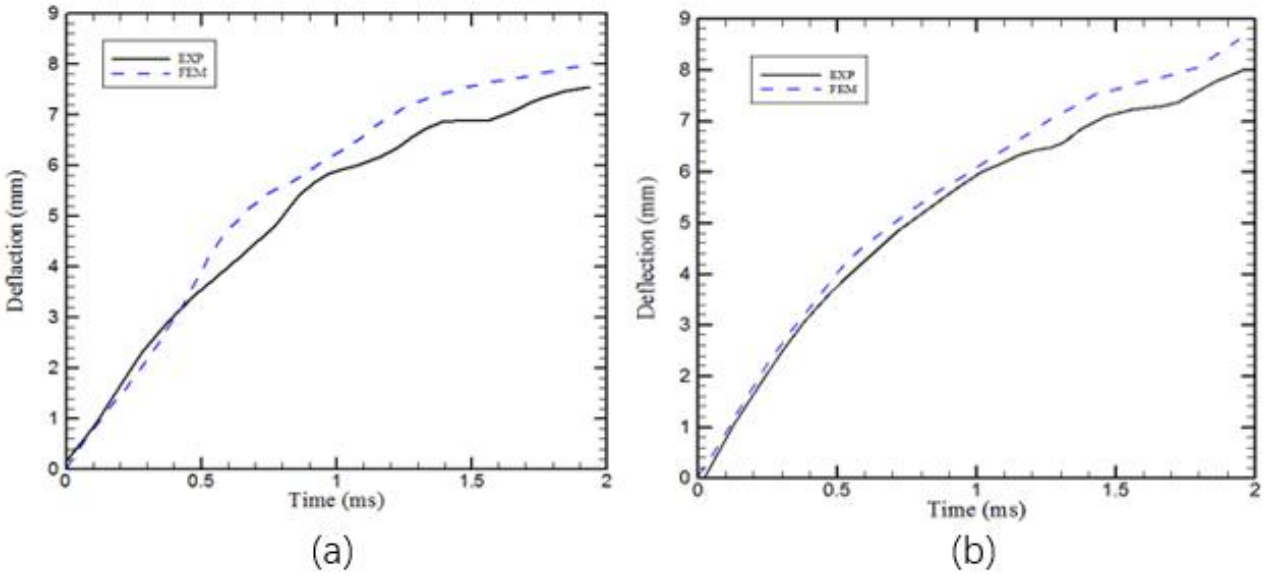

Figure 9 Time history of the middle point displacement of GFRP composite at the: (a) 1.0 m drop height with 6.7 J impact energy; (b) and a height of 1.5 m with 10 J impact energy.

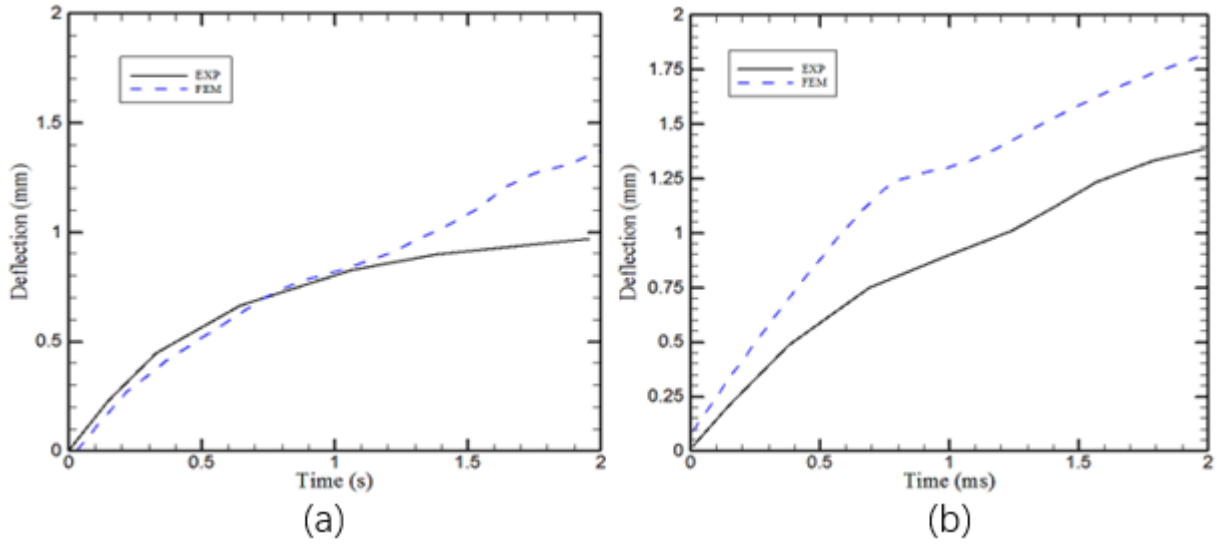

Figure 10 Time history of the middle point displacement of GLARE at (a) a height of 1.0 m with 6.7 J impact energy; (b) and a height of 1.5 m with 10 J impact energy.

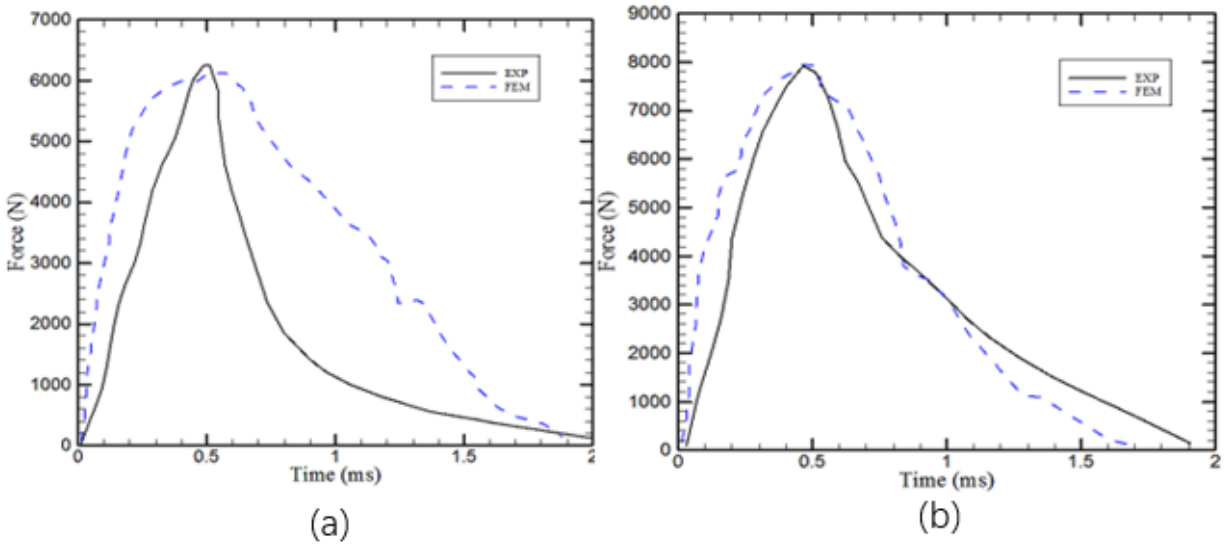

Figure 11 Time history of the contact force of GFRP composite at the: (a) height of 1 m with 6.7 J impact energy; (b) a height of 1.5 m with 10 J impact energy.

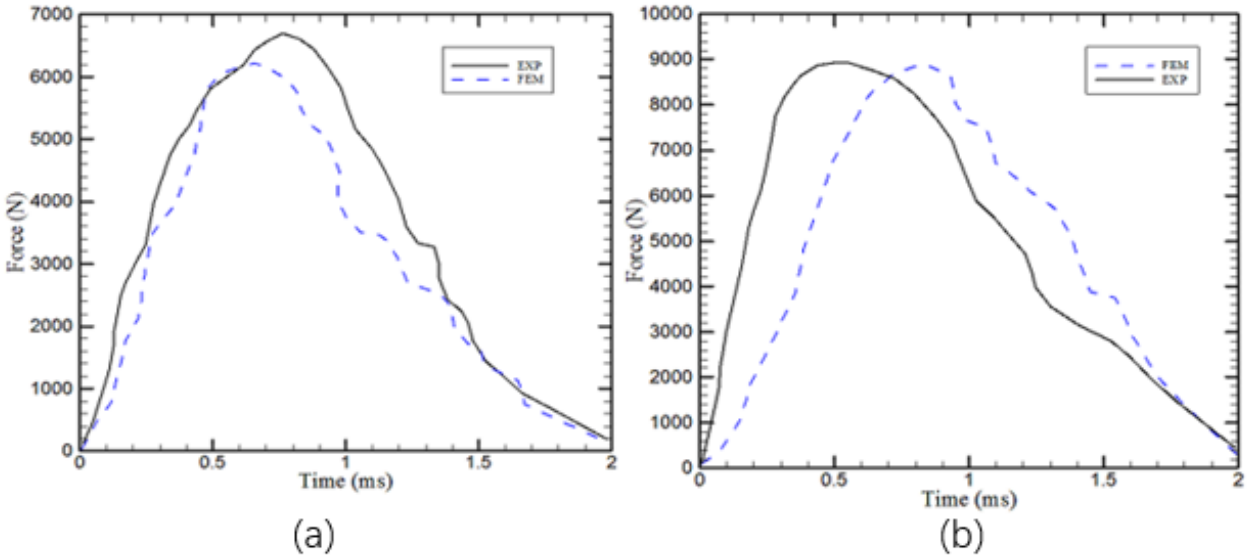

Figure 12 Time history of GLARE composite contact force at the: (a) height of 1.0 m with 6.7 J impact energy; (b) and a height of 1.5 m with 10 J impact energy.

In this section, the extent of damage to layers and fibers due to impact loads by spherical projectiles on GLARE and GFRP samples is a criterion for examining composites. The damage caused by the spherical projectile impact on the GLARE and GFRP specimens is shown in Figure 13. The results of visual inspection and finite element simulation of the composite samples after the projectile hit are demonstrated in Figure 13. At 1.0 m, the amount of damage and delamination of the GFRP sample is much less than that of 1.5 m, as shown in Figure 13(b). Furthermore, the fracture happened between layers and fibers at a height of 1.5 m. In Figure 13(c), only minor damage was inflicted on the specimen, which did not affect the sample structure. As shown in Figure 13(d), a visual examination and simulation of the specimen showed that the amount of specimen damage in GLARE composite at the height of 1.5 m was severely reduced as compared to GFRP one (Figure 13(b)), and only one layer was slightly damaged. Furthermore, as shown in Figure 13, the severity of the damage is at the top of the specimens, where the projectile strikes the specimens. Also, the crack growth and damage extended from the center of the samples to around the layers. Longitudinal stress waves of impact cause this crack growth and fractures in the sample. The Von Misses stress contour of the first layer of GFRP and GLARE for two drop heights (1 m, 1.5 m) is illustrated in Figure 14. The Von Misses stresses for the first layer are investigated after simulating the dynamic load on the laminates by a spherical projectile. The highest stress is developed in the middle of the laminates, and also, the stress of the first layer increases with increasing height.

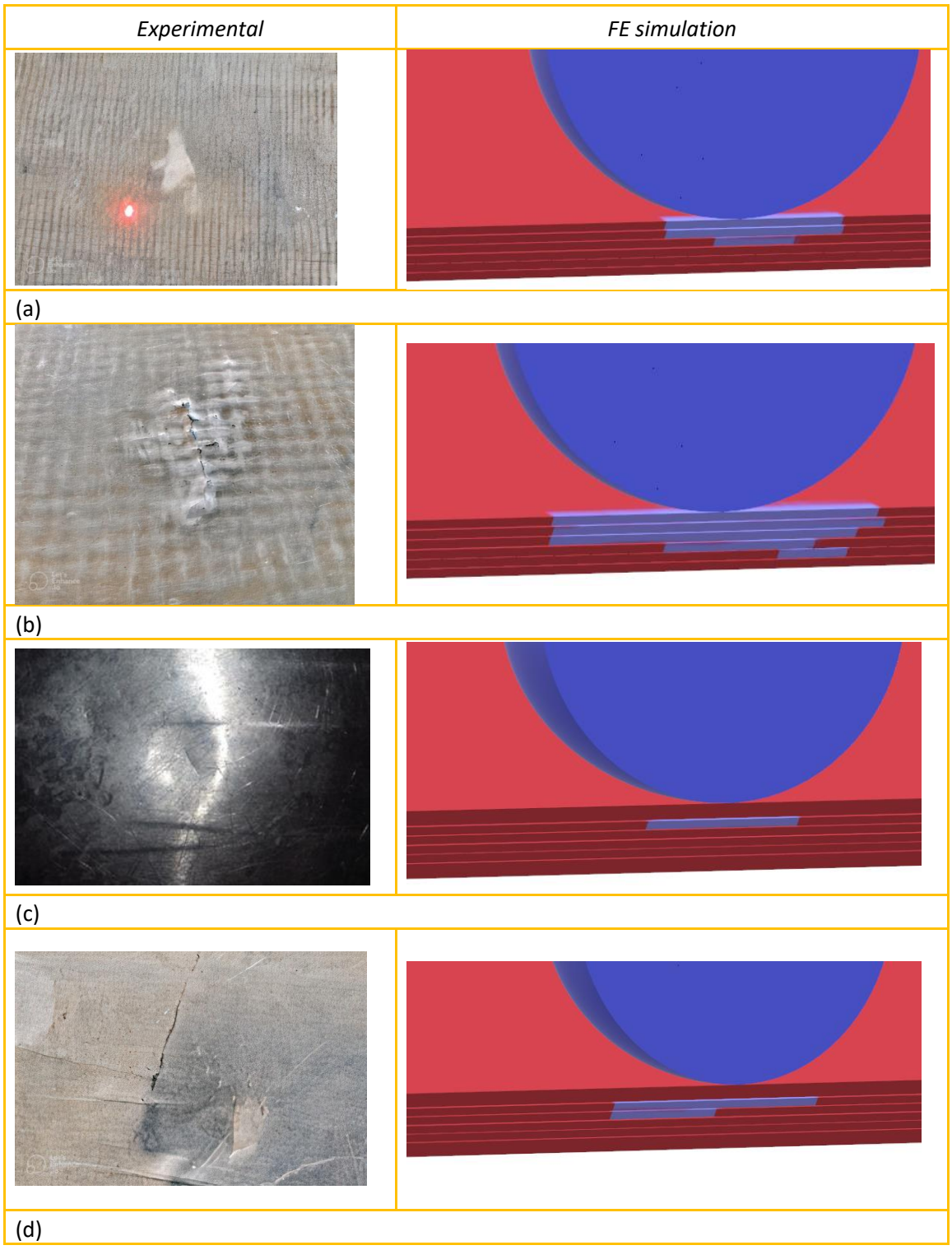

Figure 13 Damaged surface in experimental and FE results: (a) damage of GFRP composite at height of 1.0 m; (b) damage of GFRP composite at height of 1.5 m ;(c) damage of GLARE composite at height of 1.0 m; (d) damage of GLARE composite at height of 1.5 m.

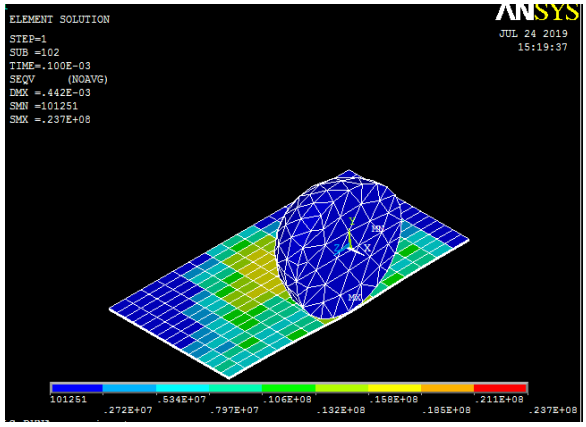

(a) GFRP

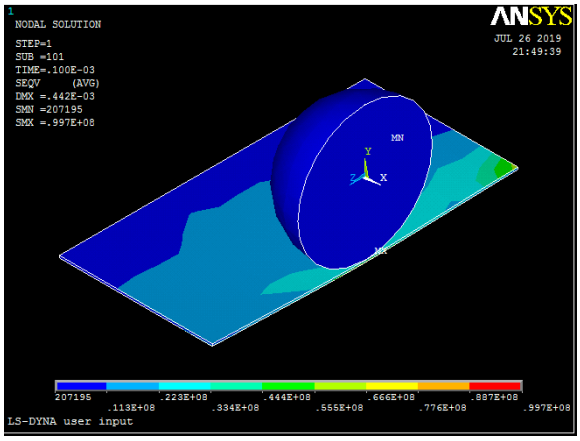

(a) GLARE

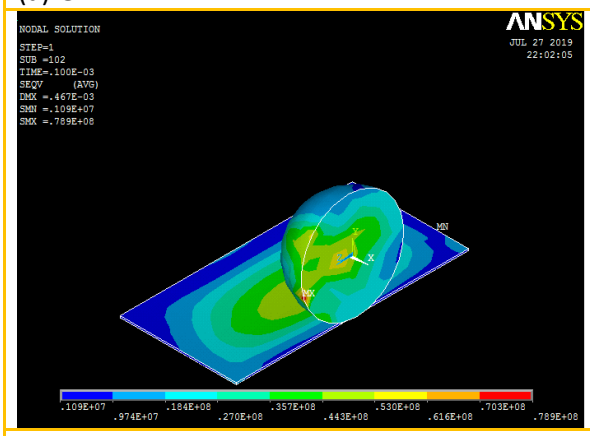

(b) GFRP

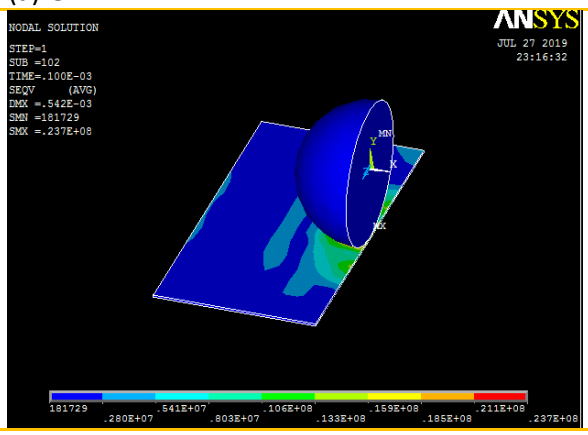

(b) GLARE

Figure 14 Von Misses stress contour of the first layer of composites: (a) at 1.0 m drop height; (b) and 1.5 m drop height.

To determine the efficiency of the numerical models, the natural frequency of the composites was obtained and compared with the experimental program and analytical methods. As shown in Figure 15, results show that the natural frequency of the GFRP composite measured by the numerical model (FE) is higher than experimental and analytical results for the first and second modes. However, similar results were obtained for the third and fourth modes. Regarding GLARE composites, general results show that the natural frequency obtained by FE models agrees well with experimental and analytical results for all modes. This clearly shows the good performance of numerical models. Generally, the results of Figure 15 show that the GLARE composite's natural frequency is significantly higher than the GFRP composite for all modes, up to 60.96%, 209.1%, 122.1%, and 130.1% improvements for the first four modes, respectively. The higher natural frequency of GLAR composites than GFRP ones can be attributed to the considerably great stiffness of GLARE composite in a ratio to its mass ($\sqrt{k/m}$).

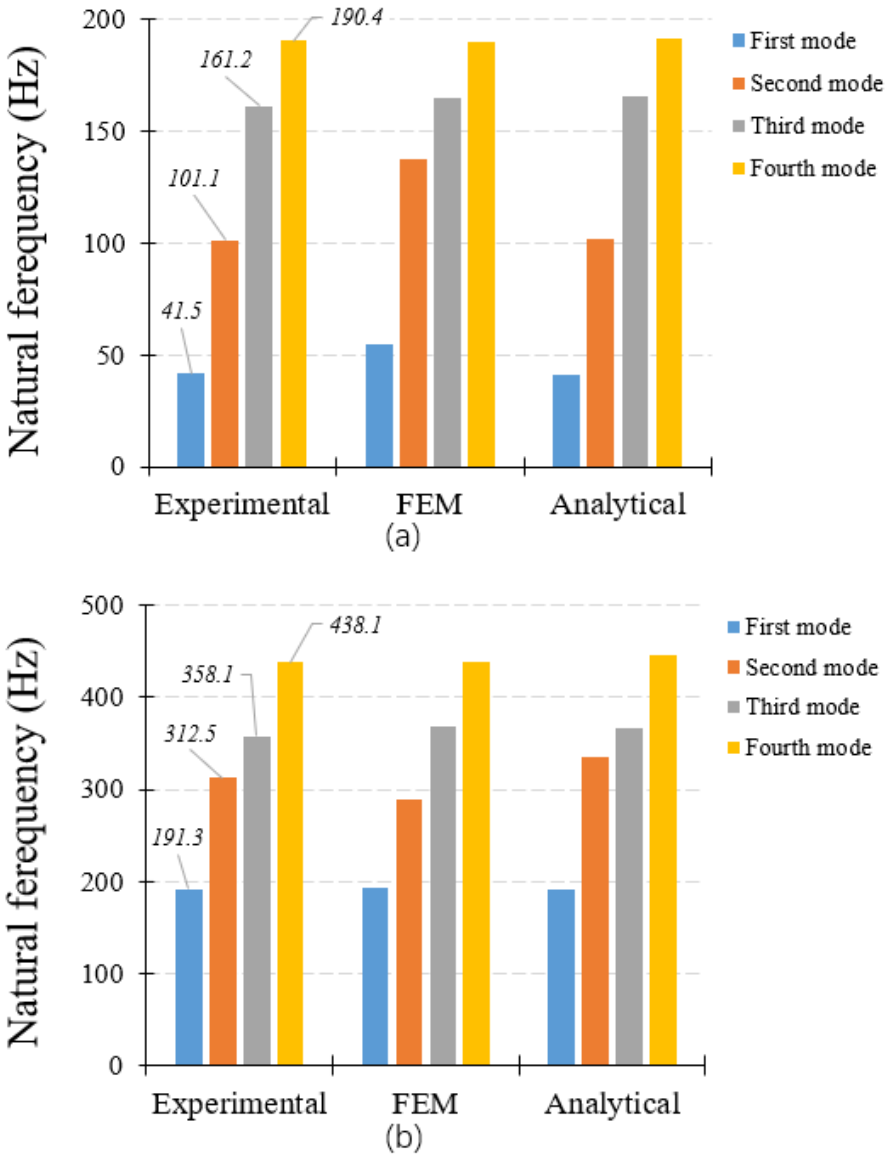

Figure 15 Natural frequency of composites: (a) GFRP; (b) GLARE.

5. Conclusion

This study investigated the behavior of GLARE and GFRP composites under a low-velocity impact test using the fully clamped boundary condition based on experimental tests and numerical analysis. A low-velocity impact test was performed at 1.0 m and 1.5 m with 6.7 j and 10 j impact energy. The GLARE samples were made by the hand lay-up method with two aluminum 7075-T6 sheets and four layers of glass fibers with dimensions of 250 × 250 × 2.8 mm, and the GFRP samples were made by using six layers of glass fibers with dimensions of 250 × 250 × 1.8 mm. The results can be summarized as follows:

1- The maximum deflection of the samples was increased by increasing the height. Also, the maximum deflection rates of GLARE and GFRP at 1.5 m were compared to 1.0 m, which increased by 34.6% and 5.6%, respectively.

2- The presence of aluminum sheets increased the impact resistance of GLARE specimens and reduced the deflection of the specimens compared to GFRP samples. The maximum deflection

of the GLARE samples at 1.0 m and 1.5 m height was reduced by 87% and 83.5% compared to the GFRP samples.

3- The presence of an aluminum sheet prevented damage to the fibers in GFRP, while GFRP samples exhibited delamination and fractures between layers.
4- After impact, the crack growth and damage were extended from the center of the samples to around the layers. Longitudinal stress waves of impact caused this crack growth and fractures in the GFRP and GLARE. And even it caused damage to the second and third layers of the GLARE composite.
5- There was good convergence and alignment between the FE simulation and experimental results. The limited error rate in the samples was due to the presence of voids, laboratory conditions, and temperature.

It is worth mentioning that although FEM obtained appropriate predictions to estimate the maximum force of GFRP and GLARE composites, more precise and practical modeling is required to be proposed by future studies to improve the performance of FEM.

Author Contributions

Conceptualization, A.A.K.; Methodology, A.A.K. & M.R.; Formal analysis, M.R. and S.S.M.; Investigation, A.A.K. and M.R.; Resources, A.A.K. & M.R.; Visualization, A.A.K. & M.R.; Validation, A.A.K. & S.S.M.; Data curation, A.A.K. & S.S.M.; Writing-original draft preparation, S.S.M. & M.R.; Writing-review and editing, S.S.M.; Supervision, A.A.K.; Project administration, A.A.K.; All authors have read and agreed to the published version of the manuscript.

Competing Interests

The authors have declared that no competing interests exist.

Reference

1. Patil NA, Mulik SS, Wangikar KS, Kulkarni AP. Characterization of glass laminate aluminium reinforced epoxy-A review. Procedia Manuf. 2018; 20: 554-562.
2. Logesh K, Raja VB, Nair VH, KM S, KM V, Balaji M. Review on manufacturing of fibre metal laminates and its characterization techniques. Int J Mech Eng Technol. 2017; 8: 561-578.
3. Azhdari S, Fakhreddini-Najafabadi S, Taheri-Behrooz F. An experimental and numerical investigation on low velocity impact response of GLAREs. Compos Struct. 2021; 271: 114123.
4. Bienias J, Jakubczak P, Dadej K. Low-velocity impact resistance of aluminium glass laminates–experimental and numerical investigation. Compos Struct. 2016; 152: 339-348.
5. Morinière FD, Alderliesten RC, Tooski MY, Benedictus R. Damage evolution in GLARE fibre-metal laminate under repeated low-velocity impact tests. Cent Eur J Eng. 2012; 2: 603-611.
6. Seyed Yaghoubi A, Liu Y, Liaw B. Low-velocity impact on GLARE 5 fiber-metal laminates: Influences of specimen thickness and impactor mass. J Aerosp Eng. 2012; 25: 409-420.
7. Rajkumar G, Krishna M, Murthy HN, Sharma S, Mahesh KV. Experimental investigation of low-velocity repeated impacts on glass fiber metal composites. J Mater Eng Perform. 2012; 21: 1485-1490.

8. Chai GB, Manikandan P. Low velocity impact response of fibre-metal laminates–A review. Compos Struct. 2014; 107: 363-381.
9. Ding Z, Wang H, Luo J, Li N. A review on forming technologies of fibre metal laminates. Int J Lightweight Mater Manuf. 2021; 4: 110-126.
10. Vermeeren C. An historic overview of the development of fibre metal laminates. Appl Compos Mater. 2003; 10: 189-205.
11. Chandrasekar M, Ishak M, Jawaid M, Leman Z, Sapuan S. An experimental review on the mechanical properties and hygrothermal behaviour of fibre metal laminates. J Reinf Plast Compos. 2017; 36: 72-82.
12. Sharma AP, Khan SH, Kitey R, Parameswaran V. Effect of through thickness metal layer distribution on the low velocity impact response of fiber metal laminates. Polym Test. 2018; 65: 301-312.
13. Khan SH, Sharma AP, Kitey R, Parameswaran V. Effect of metal layer placement on the damage and energy absorption mechanisms in aluminium/glass fibre laminates. Int J Impact Eng. 2018; 119: 14-25.
14. Sharma AP, Velmurugan R. Damage and energy absorption characteristics of glass fiber reinforced titanium laminates to low-velocity impact. Mech Adv Mater Struct. 2022; 29: 6242-6265.
15. Sharma AP, Velmurugan R. Analytical modelling of low-velocity impact response characterization of titanium and glass fibre reinforced polymer hybrid laminate composites. Thin Wall Struct. 2022; 175: 109236.
16. Sharma A, Ramachandran V. Low-velocity impact perforation response of titanium/composite laminates: Analytical and experimental investigation. Mech Based Des Struct Mach. 2021. doi: 10.1080/15397734.2021.1992778.
17. Sinmazçelik T, Avcu E, Bora MÖ, Çoban O. A review: Fibre metal laminates, background, bonding types and applied test methods. Mater Des. 2011; 32: 3671-3685.
18. Sadighi M, Alderliesten R, Benedictus R. Impact resistance of fiber-metal laminates: A review. Int J Impact Eng. 2012; 49: 77-90.
19. Zhang J, Ye Y, Qin Q, Wang T. Low-velocity impact of sandwich beams with fibre-metal laminate face-sheets. Compos Sci Technol. 2018; 168: 152-159.
20. Zhang J, Qin Q, Zhang J, Yuan H, Du J, Li H. Low-velocity impact on square sandwich plates with fibre-metal laminate face-sheets: Analytical and numerical research. Compos Struct. 2021; 259: 113461.
21. Zhang J, Zhu Y, Li K, Yuan H, Du J, Qin Q. Dynamic response of sandwich plates with GLARE face-sheets and honeycomb core under metal foam projectile impact: Experimental and numerical investigations. Int J Impact Eng. 2022; 164: 104201.
22. Zhang J, Guo H. Low-velocity impact of rectangular foam-filled fiber metal laminate tubes. Appl Math Mech. 2021; 42: 1733-1742.
23. Committee AIH. Metals handbook, Vol. 2: Properties and selection: Nonferrous alloys and special-purpose materials. Almere: ASM International; 1990. Available from: https://dl.asminternational.org/handbooks/edited-volume/14/Properties-and-Selection-Nonferrous-Alloys-and.

24. Seifoori S, Izadi R, Yazdinezhad A. Impact damage detection for small-and large-mass impact on CFRP and GFRP composite laminate with different striker geometry using experimental, analytical and FE methods. Acta Mech. 2019; 230: 4417-4433.
25. Seifoori S, Parrany AM, Mirzarahmani S. Impact damage detection in CFRP and GFRP curved composite laminates subjected to low-velocity impacts. Compos Struct. 2021; 261: 113278.
26. Taheri-Behrooz F, Shokrieh M, Yahyapour I. Effect of stacking sequence on failure mode of fiber metal laminates under low-velocity impact. Iran Polym J. 2014; 23: 147-152.
27. Fakhreddini-Najafabadi S, Torabi M, Taheri-Behrooz F. An experimental investigation on the low-velocity impact performance of the CFRP filled with nanoclay. Aerosp Sci Technol. 2021; 116: 106858.
28. Hashin Z. Fatigue failure criteria for unidirectional fiber composites. Philadelphia, PA: Pennsylvania Univ Philadelphia Dept of Materials Science and Engineering; 1980.